



HAL
open science

The Gas-Phase Microwave Spectrum of Sabinene Revisited Reveals New Structural Parameters

Mhamad Chrayteh, Thérèse Huet, Pascal Dréan

► **To cite this version:**

Mhamad Chrayteh, Thérèse Huet, Pascal Dréan. The Gas-Phase Microwave Spectrum of Sabinene Revisited Reveals New Structural Parameters. *Journal of Molecular Structure*, 2021, pp.130515. 10.1016/j.molstruc.2021.130515 . hal-03206451

HAL Id: hal-03206451

<https://hal.science/hal-03206451>

Submitted on 24 May 2023

HAL is a multi-disciplinary open access archive for the deposit and dissemination of scientific research documents, whether they are published or not. The documents may come from teaching and research institutions in France or abroad, or from public or private research centers.

L'archive ouverte pluridisciplinaire **HAL**, est destinée au dépôt et à la diffusion de documents scientifiques de niveau recherche, publiés ou non, émanant des établissements d'enseignement et de recherche français ou étrangers, des laboratoires publics ou privés.



Distributed under a Creative Commons Attribution - NonCommercial 4.0 International License

The Gas-Phase Microwave Spectrum of Sabinene Revisited Reveals New Structural Parameters

Mhamad Chrayteh*, Thérèse R. Huet, Pascal Dréan*

University of Lille, CNRS, UMR 8523 - PhLAM - Physique des Lasers, Atomes et Molécules, F-59000 Lille, France

Abstract

The rotational spectrum and the gas phase structure of the bicyclic monoterpene sabinene ($C_{10}H_{16}$ -4-methylene-1-(1-methylethyl)bicyclo[3.1.0]hexane), a main biogenic volatile organic compound precursor of secondary organic aerosols, was reinvestigated theoretically and experimentally employing a combination of quantum chemical calculations and Fourier transform microwave spectroscopy coupled to a supersonic jet expansion in the 2 – 20 GHz frequency region. The spectra of the parent species and of all singly substituted ^{13}C isotopologues have been analysed in natural abundance. The 11 sets of rotational constants allowed to determine the partial substitution and effective structures of sabinene. They are in fair agreement with the optimized ones at the B3LYP, M06-2X and MP2 levels associated with the 6-311++G(d,p) basis set. Our results correct the conclusions issued from the early low-resolution study of Kisiel and Legon [J. Am. Chem. Soc., 100 (1978), 8166-8169]. The dihedral angle ϕ defining the boat arrangement of the five-membered ring was determined to be 55° while we determined it to be 26.9° . The structure of sabinene reveals the same structural parameters as bicyclo[3.1.0]hexane and two of its derivatives bicyclo[3.1.0]hexan-2-one and 2, 4-dioxabicyclo[3.1.0]hexan-3-one.

Keywords: Sabinene ; microwave spectroscopy ; molecular structure

1. Introduction

Volatile organic compounds (VOCs) emitted mostly by natural sources, play an important and crucial role in the chemistry of the lower troposphere. Monoterpenes consisting of two isoprene C_5H_8 units are a family of molecules abundantly emitted by vegetation and in large quantities.[1, 2] They participate in many oxidation reactions to produce precursors of secondary organic aerosols (SOAs).[3, 4, 5, 6, 7] They affect the environment, climate, and human health.[8] Sabinene ($C_{10}H_{16}$ -4-methylene-1-(1-methylethyl)bicyclo[3.1.0]hexane) shown in Fig. 1a is a bicyclic monoterpene with an exocyclic double bond. In Europe, it is emitted in the troposphere by trees such as *Quercus ilex*, *Betula pendula*, and *Fagus sylvatica* [9, 10, 11] with an estimated flux of 20 Tg yr^{-1} . [12] Sabinene is highly reactive towards ozone [13] and hydroxyl radicals OH [14] and produces many potential precursors of SOAs such as sabinone, formaldehyde, and formic acid.[15, 16, 17, 18] Apart from being a main biogenic volatile organic compound, sabinene has some medicinal benefits as an anti-inflammatory. [19] It can also be used as perfume additives and flavorings,[20] and enters in the oil composition of the black pepper.[21]

A detailed description of the structure of sabinene is essential to accurately describe its role in the oxidation mechanisms in which it participates. The bicyclic structure is characterized by the dihedral angles τ and ϕ shown in Fig. 1b, which define the boat arrangement of the molecule. Rotational spectroscopy of monoterpenes dates over 40 years when six different molecules including sabinene, sharing the skeleton of bicyclo[3.1.0]hexane, were investigated.[22] The technique of low-resolution microwave spectroscopy employed therein only allowed the determination of the $(B + C)$ combination of rotational constants of the parent species. The dihedral angle ϕ was determined to be 55° using many assumptions. Indeed, most of the bond lengths and bond angles were taken from the studies of bicyclo[3.1.0]hexane,[23] and of bicyclo[3.1.0]hexan-3-

*Corresponding author

Email addresses: mhamad.chrayteh@univ-lille.fr (Mhamad Chrayteh), pascal.drean@univ-lille.fr (Pascal Dréan)

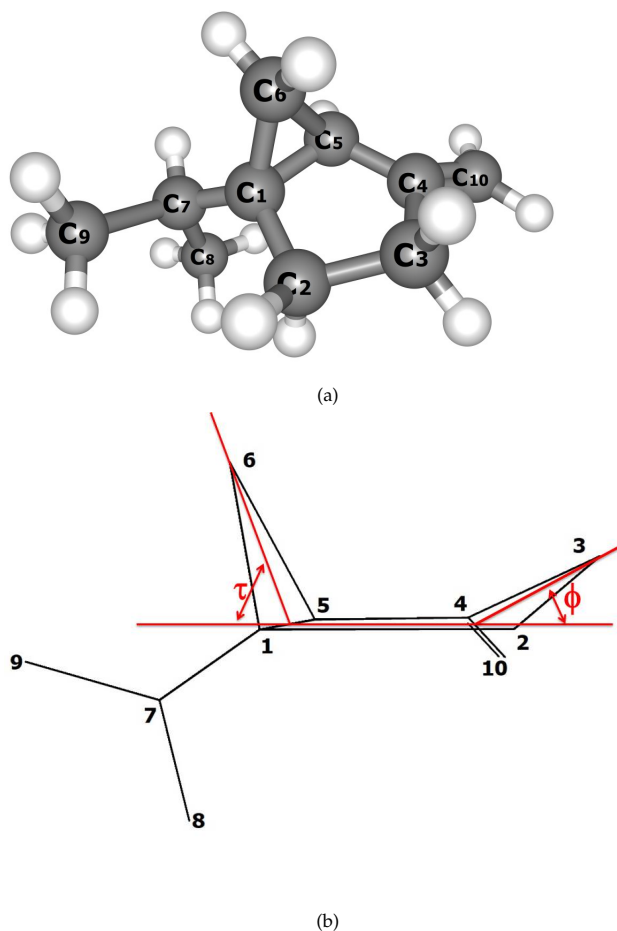


Figure 1: (a) The molecular structure of sabinene calculated at the MP2/6-311++G(d,p) level, and the numbering of the carbon atoms.(b) The carbon atom skeleton of sabinene showing the dihedral angles τ and ϕ which define the conformation of the bicyclic system.

one.[24] This experimental value of ϕ is quite high compared to the values in other bicyclo[3.1.0]hexane derivatives.[25] In bicyclo[3.1.0]hexane itself, the value of ϕ was determined to be 18.8° , [23] in agreement with recent calculations.[25] A new investigation of the rotational spectrum of sabinene is then required in order to clarify its molecular structure. This is made possible thanks to advances in computational chemistry, resolution and sensitivity of microwave spectroscopy coupled to supersonic expansions, which enables the observation of the spectra of isotopic species in natural abundances, necessary to determine the molecular geometry. For example, bicyclic structures based on bicyclo[2.2.1]heptane like fenchone,[26] camphor,[27] and camphene,[28] and on bicyclo[3.1.1]heptane like α -pinene,[29] β -pinene, nopinone,[30] myrtenal [31] and verbenone [32] were studied by high resolution rotational spectroscopy. In this work, the microwave spectrum of sabinene has been re-investigated using a cavity-based Fourier-transform microwave spectrometer coupled to a supersonic expansion in the 2 – 20 GHz frequency range. The main objective of our study is to calculate the r_s and r_0 structures through the analysis of the spectra of the ^{13}C isotopologues in natural abundance. These structures are compared with the former parameters determined for sabinene and also with those of bicyclo[3.1.0]hexane (BCH),[23] bicyclo[3.1.0]hexan-2-one (BCHO)[33] and 2,4-dioxabicyclo[3.1.0]hexan-3-one.[34]

2. Computational

The quantum chemical calculations were performed using the Gaussian 16 Package B.01 software [35] implemented in the High-Performance Computing Linux cluster of the PhLAM laboratory. Geometry optimization of sabinene was done by using density functional theory, with the B3LYP [36] and M06-2X functionals,[37] and *ab initio* calculations using the Møller-Plesset perturbation theory to second order (MP2)[38] combined with the 6-311++G(d,p) Pople's triple- ζ basis set with diffuse and polarization functions. Pople's 6-311G++(3df,2pd) basis set was also used with MP2 method. The quartic centrifugal distortion constants in the harmonic approximation were calculated at the corresponding optimized geometry.

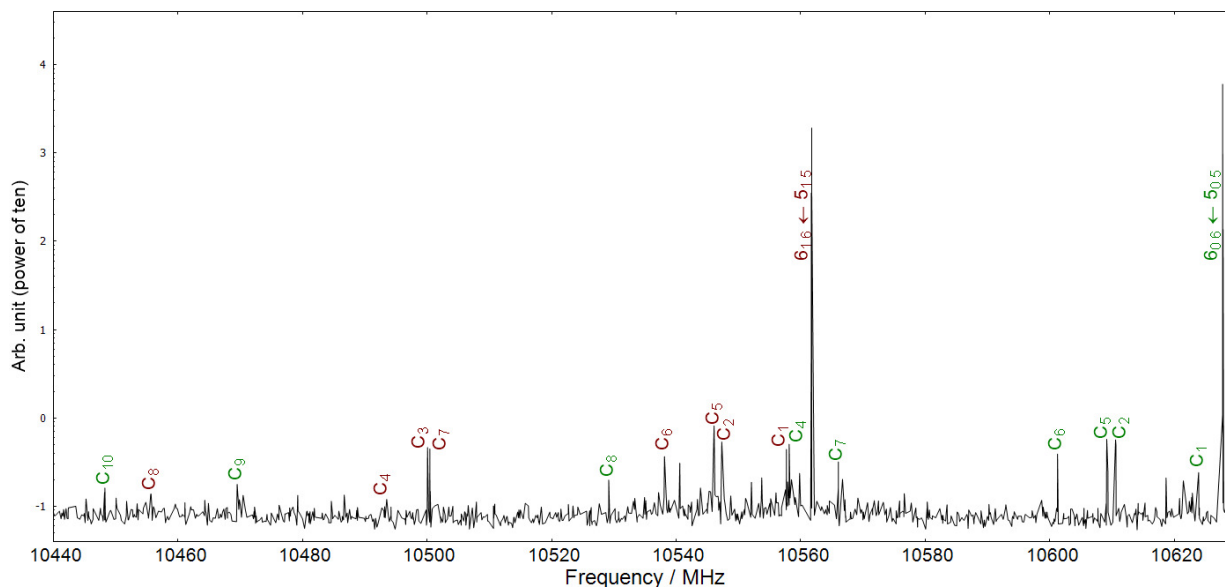


Figure 2: Part of the spectrum of sabinene from 10440 to 10630 MHz, showing the $6_{16} \leftarrow 5_{15}$ (red) and $6_{06} \leftarrow 5_{05}$ (green) lines of the parent species and the corresponding observed red-shifted lines of the isotopic species, recorded at a resolution of 15 kHz. The intensity axis is in an arbitrary logarithmic scale.

3. Experimental details

The pure rotational spectrum of sabinene was recorded in the microwave range 2-20 GHz using two cavity-based Fourier transform spectrometers differing by the diameter of their mirrors. One of them with a mirror of diameter 0.4 m is adapted for measurements of lines between 8 and 20 GHz, while the other with a mirror of diameter 0.7 m is more efficient for measurements below 9 GHz.[39, 40]

Sabinene (0.2 mL, Sigma-Aldrich-75%) placed into the reservoir of an injector[41] and heated at 338 K, was pressurized under 3 bar of neon used as carrier gas. The gas mixture was injected into the Fabry-Pérot cavity through a short opening (800 μs) of an orifice of 1 mm internal diameter (Iota One, General Valve) at a repetition rate of 1 Hz to create a supersonic jet with a rotational temperature of a few Kelvin. The molecules were polarized by 2 μs microwave pulses carrying an energy adjusted to be close to the $\pi/2$ condition.

In the detection setup, Free-Induction Decays (FIDs) were detected at the heterodyne frequency of 30 MHz and digitized at a sampling rate of 120 MHz by an acquisition device. The lines of the parent species were digitized over 65 536 to 131 072 points which led to a frequency grid of 1.84 to 0.92 kHz. Most of the lines of the ^{13}C isotopic species were digitized over 65 536 points. Hundreds of FIDs were accumulated for the less intense lines (in particular those of the isotopic species) in order to improve their signal-to-noise ratio. Lines were observed as two Doppler components, due to the coaxial arrangement of the supersonic jet and of the mirrors. The frequencies were determined by averaging the frequencies of the two Doppler components.

4. Experimental results and discussion

4.1. Rotational spectrum

The rotational spectrum of sabinene was assigned in light of equilibrium computed rotational constants and electric dipole moment components listed in Table 1. Sabinene is a near prolate asymmetric rotor with a Ray's asymmetry parameter value $\kappa = -0.97$. The values of the components of the electric dipole moment of sabinene are small. The value along the a inertial axis is 0.73 D, while the values of the b and c -components are much lower, respectively 0.21 D and 0.09 D, as calculated at the MP2/6-311++G(d,p) level. The rotational spectrum of sabinene is expected to be composed of rather intense a -type and weak b -type lines. The c -type lines are not expected to be easily observable. A portion of the experimental spectrum is displayed in Fig. 2, showing the lines corresponding to the $6_{16} \leftarrow 5_{15}$ and $6_{06} \leftarrow 5_{05}$ transitions of the parent and of the singly substituted ^{13}C isotopic species.

Table 1: Experimental ground state and calculated equilibrium rotational and quartic centrifugal distortion constants of sabinene.

Parameter	Exp. value	B3LYP ^a	M06-2X ^a	MP2 ^a	MP2 ^b
A / MHz	2457.962 69(25)	2454.66	2465.98	2447.44	2468.87
B / MHz	898.808 31(13)	888.36	904.74	905.62	913.72
C / MHz	874.178 34(12)	865.81	879.56	876.77	884.92
Δ_J / kHz	0.059 70(32)	0.0535	0.0613	0.0622	0.0641
Δ_{JK} / kHz	-0.2170(17)	-0.0177	-0.2390	-0.2432	-0.2504
Δ_K / kHz	0.844(21)	0.7309	0.8678	0.8617	0.8871
δ_J / kHz	0.012 80(19)	0.0113	0.0140	0.0140	0.0143
δ_K / kHz	0.321(57)	0.2232	0.2382	0.1442	0.1590
$ \mu_a $ / D	y	0.86	0.81	0.73	0.77
$ \mu_b $ / D	y	0.29	0.27	0.21	0.23
$ \mu_c $ / D	n	0.08	0.09	0.09	0.08
N_{lines}	93	-	-	-	-
σ_{fit} / kHz	1.38	-	-	-	-
κ	-0.969	-0.972	-0.968	-0.963	-0.964
	Our work	Previous work[22]			
$B+C$ / MHz	1772.986 65(25)	1772.0(6)			

Basis sets : ^a 6-311++G(d,p) ; ^b 6-311++G(3df,2pd).

A survey scan was made from 7000 to 7100 MHz in order to identify the strong ^{type} $\Delta J_{\Delta K_a \Delta K_c} = {}^a R_{01}$ lines. Four intense lines were observed at 7042.1, 7089.0, 7091.7 and 7094.6 MHz. They were respectively ascribed to the $4_{14} \leftarrow 3_{13}$, $4_{04} \leftarrow 3_{03}$, $4_{23} \leftarrow 3_{22}$ and $4_{22} \leftarrow 3_{21}$ transitions. A very few c -type lines could be observed at a resolution of 15 kHz, but they were not measurable at higher resolutions. They were not considered in our analysis. We finally obtained a collection of 93 measured lines of a and b types, from $J = 2$ up to $J = 11$ and $K_a = 7$. Watson's rotational Hamiltonian including centrifugal distortion up to the quartic terms set up in the A reduction and I' representation as implemented in the Pickett's suite of programs (SPFIT, SPCAT) was used to fit the measured transitions.[42] The resulting experimental ground state rotational and centrifugal distortion constants are listed in Table 1. They are accurately determined despite δ_K carries a relatively large error due to the limited range of values of J , K_a and K_c accessible in the microwave region. The value of $(B + C)$, 1772.986 65(25) MHz, is in very good agreement with that reported by Kisiel and Legon, [22] of 1772.0(6) MHz. The computed equilibrium rotational constants are close to the effective experimental ones, with deviations of less than 1%, slightly higher for those employing large basis sets for which the deviations reach 1.7% for the B constant calculated at the MP2/6-311++G(3df,2pd) level. It should be noted that using a DFT method like M06-2X provides accurate rotational and centrifugal distortion constants, even at the harmonic approximation.

Once the spectrum of the parent species of sabinene was analysed, the rotational constants of the ten ¹³C mono-substituted isotopic species were predicted by the CORSCL program [43] using the optimized geometry at the MP2/6-311++G(d,p) level as input (see Listing S1 of the Supplementary Material). The lines of the isotopic species were found rather close to their predicted frequencies (± 2 MHz for $J = 6$). Their intensity were generally weak and only a -type transitions could be measured. They are collected in Tables S2 to S11 of the Supplementary Material. In order to improve the fit of the transitions, it was necessary to set free Δ_J while the remaining quartic centrifugal constants Δ_{JK} , Δ_K , δ_J and δ_K were fixed to the values of the parent species. The spectroscopic constants of the ten isotopologues are listed in Table 2. The determination of the A constant suffers from the lack of b -type transitions.

Table 2: Spectroscopic parameters of the ten singly substituted ^{13}C isotopic species of sabinene ^a.

	$^{13}\text{C}_1$	$^{13}\text{C}_2$	$^{13}\text{C}_3$	$^{13}\text{C}_4$	$^{13}\text{C}_5$
A / MHz	2456.78(21)	2435.35(11)	2437.476(92)	2457.57(11)	2446.54(17)
B / MHz	898.50687(16)	896.755152(93)	893.113882(92)	892.85631(15)	896.56089(18)
C / MHz	873.83441(16)	873.24003(11)	869.21054(13)	868.48755(14)	873.16857(16)
Δ_J / kHz	0.0593(16)	0.0598(12)	0.0638(11)	0.0583(14)	0.0573(19)
N_{lines}	15	14	14	14	14
σ_{fit} / kHz	1.55	0.91	0.91	2.09	1.49
	$^{13}\text{C}_6$	$^{13}\text{C}_7$	$^{13}\text{C}_8$	$^{13}\text{C}_9$	$^{13}\text{C}_{10}$
A / MHz	2424.061(80)	2455.31(13)	2423.310(71)	2453.35(10)	2448.024(96)
B / MHz	895.946714(80)	893.53196(14)	892.48636(10)	885.53158(13)	884.077782(91)
C / MHz	872.486403(72)	869.12676(13)	864.57419(11)	861.04291(13)	859.03711(10)
Δ_J / kHz	0.05916(75)	0.0597(13)	0.05993(96)	0.0575(14)	0.0578(11)
N_{lines}	14	13	15	13	15
σ_{fit} / kHz	0.70	1.40	0.99	0.98	0.95

^a Δ_{JK} , Δ_K , δ_J , and δ_K were fixed to the values of the parent species (see Table 1).

4.2. Structure

The absolute values of the coordinates of each substituted atom of sabinene (in our case the ten carbon atoms of carbon) were calculated from the slight variations of the planar moments induced by the substitution. They are called substitution or r_s coordinates and obtained by solving the Kraitchman's equations [44] as implemented in the Kisiel's KRA program. [45] The substitution coordinates are purely experimental ones and can be used as benchmark for validation of the expected structure. The error on a coordinate z is the result of two contributions: the propagation of the uncertainties on the rotational constants, dominated by the error suggested by Costain, *i.e.* $\delta z = 0.0015 \text{ \AA}^2 / |z|$. [46] The r_s coordinates along with those issued from the MP2/6-311++G(d,p) calculation are presented in Table 3. There is no way to confuse any carbon with another one, even considering only the absolute values of the coordinates. The r_s coordinates were given the signs of the MP2 ones. The coordinate of C_2 along the a axis, and of C_4 and C_9 along the c axis were returned as imaginary numbers, which means they are close to 0, as confirmed by the MP2 calculation. Experimental and calculated coordinates are generally in very good agreement with each other except in the case of C_1 . Small coordinates, like those of C_1 , suffer from the neglect of vibrational contributions in Kraitchman's equations. The errors on the coordinates are then underestimated, and the coordinates themselves are likely meaningless. Such failure was recently observed by Minei and Cooke in their study on fluorinated cyclopentanes, [47] attributed to low normal modes of vibrations occurring in large molecules. [48] In sabinene, according to the MP2/6-311++G(d,p) calculation, the three lowest normal modes are located at $\approx 60 \text{ cm}^{-1}$, $\approx 99 \text{ cm}^{-1}$ and $\approx 164 \text{ cm}^{-1}$. The lowest vibrational mode implies a deformation which greatly affects the position of all the carbon atoms, except C_5 . Nevertheless, the expected structure of sabinene is confirmed.

A partial r_s structure of the carbon skeleton of sabinene was calculated using the substitution coordinates of each atom of carbon with the imaginary ones replaced by their MP2 values. We have also used the MP2 coordinates of C_1 instead of its ill-determined r_s . The coordinates borrowed from *ab initio* calculations were given an uncertainty of 0. The structural parameters involving C_1 are then not purely experimental parameters and the corresponding uncertainties are underestimated. The utility software EVAL [45] was employed to facilitate the calculations. A ground state or effective structure called r_0 was also derived by fitting internal structural parameters to all available ground-state rotational constants. The STRFIT program written by Kisiel was used. [45, 49] Additional informations were necessary, like the parameters involving the hydrogen atoms taken from the MP2/6-311++G(d,p) optimized geometry. Over a total of 24 internal structural parameters, 21 were fitted (9 bond lengths, 6 bond angles and 6 dihedral angles), with a standard deviation of 0.0091 u\AA^2 (the STRFIT output is given in Listing S2 of the Supplementary Material). Two bond angles and one dihedral angle, namely

Table 3: Substitution and theoretical coordinates (in Å) of the ten ^{13}C atoms of sabinene along the a , b and c principal axis.

Atom	a		b		c	
	r_s	MP2 ^a	r_s	MP2 ^a	r_s	MP2 ^a
C ₁	-0.2833(95)	-0.436	-0.187(15)	-0.275	0.124(22)	0.189
C ₂	0.017-i	0.072	-0.7571(35)	-0.743	-1.1591(25)	-1.173
C ₃	1.6058(15)	1.608	-0.8279(29)	-0.838	-1.0305(25)	-1.023
C ₄	1.9407(14)	1.939	0.192(15)	0.190	0.059-i	0.042
C ₅	0.7482(52)	0.766	0.323(12)	0.292	0.9279(42)	0.940
C ₆	0.144(16)	0.122	-0.9905(22)	-1.026	1.3806(17)	1.366
C ₇	-1.8000(17)	-1.802	0.3639(86)	0.370	0.305(10)	0.312
C ₈	-1.9278(11)	-1.908	1.6388(13)	1.655	-0.5451(43)	-0.515
C ₉	-2.90793(89)	-2.909	-0.6314(42)	-0.622	-0.037-i	-0.063
C ₁₀	3.06225(83)	3.046	0.9234(28)	0.951	0.086(31)	0.095

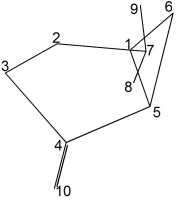
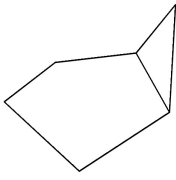
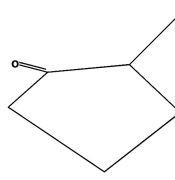
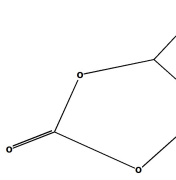
^a 6-311++G(d,p).

$\angle(\text{C}_6\text{C}_5\text{C}_1)$, $\angle(\text{C}_{10}\text{C}_4\text{C}_3)$ and $\tau(\text{C}_9\text{C}_7\text{C}_1\text{C}_6)$, could not be determined. They were fixed at the value of the MP2/6-311++G(d,p) optimized geometry. The mass-dependent structure r_m accounting for the rovibrational correction could not be determined despite several attempts. The r_s , r_0 and MP2/6-311++G(d,p) structural parameters are listed in Table 4.

A first comparison between the experimental r_s structure and the MP2 optimized one shows that they are in very good agreement. The main difference between r_s and MP2 bond lengths concern the $r(\text{C}_5-\text{C}_6)$ one, but with a very acceptable absolute deviation of 0.012 Å. Comparison of structural parameters of sabinene with those of the related species BCH and BCHO reveals a close agreement, even if the $-\text{C}=\text{C}$ double bond in sabinene is replaced by a $-\text{C}=\text{O}$ bond in BCHO. For instance, the $r_s(\text{C}_4-\text{C}_5)$ bond length is 1.491(5) Å in sabinene and the corresponding bond length in BCHO was determined to be 1.470 Å (see Table 4). Bond angles are known to be accurately determined by chemical quantum calculations, generally within a few tenths of degree. This is the case for all the bond angles listed in Table 4, except for one of them. Indeed, the difference of 3.8° between the r_s and MP2 values of the $\angle(\text{C}_4\text{C}_5\text{C}_6)$ is surprisingly high. The r_0 structural parameters are also in agreement with the optimized MP2 structure, although a bit less, but in this case we compare ground state and equilibrium structures. The optimized structures obtained with other methods are reported in S12. Deviations are a bit higher, especially considering the M06-2X optimized structure, but they nevertheless remain in good agreement with the r_s structure.

In the early calculated structure,[22] the carbon atoms C₁, C₂, C₄ and C₅ were assumed to be coplanar. Our results show that the atoms C₁, C₂, C₄ and C₅ are not strictly coplanar. Indeed, the dihedral angle $\tau(\text{C}_1\text{C}_2\text{C}_4\text{C}_5)$ has a MP2 value of 0.74°, and an effective value of 0.73(6)°. The meaning of τ and ϕ is then partially lost since they can not be strictly defined with respect to a plane. The dihedral angle τ (see Fig. 1b) can be calculated using the $\tau(\text{C}_4\text{C}_5\text{C}_1\text{C}_6)$ or $\tau(\text{C}_2\text{C}_1\text{C}_5\text{C}_6)$ dihedral angles since they are supplementary angles. The same holds for the dihedral angle ϕ obtained from $\tau(\text{C}_1\text{C}_2\text{C}_4\text{C}_3)$ or $\tau(\text{C}_5\text{C}_4\text{C}_2\text{C}_3)$. The value of τ , generally comprised between 63° and 70°,[25] is a characteristic of compounds based on bicyclo[3.1.0]hexane (see Table 4). The lowest value of 63° was obtained for BCH and for sabinene, we have obtained the highest value of 70.97°, in fair agreement with the *ab initio* value of 69.29°. The updated experimental value of τ differs by $\approx 3^\circ$ from the value borrowed from BCHO used in the former determination of ϕ . The structural parameters of the three-membered ring and those of the isopropyl and methyl groups were fixed to the values obtained for bicyclo[3.1.0]hexan-3-one and to standard values.[24] Within these assumptions, and having only the $(B + C)$ value, the ring-puckering angle ϕ defined in Fig. 1b was determined to be 55°. The experimental values of ϕ we have obtained are in the range 26.52(91) to 27.61(60)° according to the chosen data (r_s or r_0), compatible with the *ab initio* value of 29.33°. The reason why the determination of ϕ by Kisiel and Legon led to a very different value than ours is not elucidated.

Table 4: Structural parameters of the carbon skeleton of sabinene determined experimentally and theoretically, and comparison with those of related species.

	sabinene			bicyclo[3.1.0] hexane ^a	bicyclo[3.1.0] hexan-2-one ^b	2, 4-dioxabicyclo[3.1.0] hexan-3-one ^c	
							
Parameter	r_s	r_0^d	Ref. [22]	MP2			r_s
$r(C_1-C_2)/\text{\AA}$	1.519(2)	1.512(12)	1.534 ^f	1.527	-	1.534	—
$r(C_1-C_5)/\text{\AA}$	1.519(6)	1.508(12)	1.519 ^f	1.527	1.513	1.519 ^f	1.497(16)
$r(C_1-C_6)/\text{\AA}$	1.506(6)	1.495(13) ^e	1.510 ^f	1.504	1.513	1.510 ^f	1.522(15)
$r(C_1-C_7)/\text{\AA}$	1.510(4)	1.537(10)	1.541 ^f	1.516	—	—	—
$r(C_2-C_3)/\text{\AA}$	1.541(2)	1.577(18) ^e	1.541 ^f	1.546	-	1.541 ^f	—
$r(C_3-C_4)/\text{\AA}$	1.518(10)	1.510(9)	1.529 ^f	1.516	1.530	1.529 ^f	—
$r(C_5-C_6)/\text{\AA}$	1.515(12)	1.528(9)	1.510 ^f	1.527	-	1.510 ^f	1.522(15)
$r(C_4-C_5)/\text{\AA}$	1.491(5)	1.499(7)	1.529 ^f	1.481	1.530	1.470	—
$r(C_7-C_8)/\text{\AA}$	1.538(10)	1.544(9)	1.541 ^f	1.532	—	—	—
$r(C_7-C_9)/\text{\AA}$	1.534(7)	1.531(7)	1.541 ^f	1.532	—	—	—
$r(C_4=C_{10})/\text{\AA}$	1.340(8)	1.339(6)	1.338 ^f	1.344	—	—	—
$\angle(C_5C_1C_6)/^\circ$	60.1(5)	61.2(7) ^e	59.81 ^f	60.5	-	-	60.3(13)
$\angle(C_2C_1C_5)/^\circ$	107.2(2)	109.60(91)	108.9 ^f	106.9	108.1	108.9 ^f	—
$\angle(C_5C_1C_7)/^\circ$	120.0(5)	119.7(7) ^e	118.3 ^f	120.8	—	-	—
$\angle(C_2C_1C_7)/^\circ$	120.3(4)	118.2(13)	118.3 ^f	120.2	—	-	—
$\angle(C_2C_1C_6)/^\circ$	115.0(4)	116.6(7) ^e	-	114.9	-	-	—
$\angle(C_1C_5C_6)/^\circ$	59.5(5)	59.0(6) ^e	59.81 ^f	59.0	-	-	60.3(13)
$\angle(C_1C_5C_4)/^\circ$	107.5(4)	106.5(6) ^e	108.9 ^f	107.4	-	108.9 ^f	—
$\angle(C_4C_5C_6)/^\circ$	112.5(4)	114.5(9)	-	116.3	-	-	—
$\angle(C_1C_6C_5)/^\circ$	60.3(2)	59.8(4) ^e	60.42 ^f	60.5	-	-	58.5(15)
$\angle(C_1C_2C_3)/^\circ$	105.9(2)	103.7(7) ^e	106.0 ^f	105.2	100.8	-	—
$\angle(C_1C_7C_8)/^\circ$	112.5(4)	112.1(5)	109.44 ^f	112.0	—	—	—
$\angle(C_1C_7C_9)/^\circ$	111.1(5)	111.4(6)	109.44 ^f	110.9	—	—	—
$\angle(C_8C_7C_9)/^\circ$	110.2(5)	110.5(4) ^e	109.44 ^f	111.2	—	—	—
$\angle(C_3C_4C_5)/^\circ$	107.6(6)	108.0(5)	106.5 ^f	107.4	-	-	—
$\angle(C_5C_4C_{10})/^\circ$	127.0(13)	125.6(7) ^e	-	126.1	—	—	—
$\angle(C_3C_4C_{10})/^\circ$	125.1(11)	126.2(5) ^e	-	126.2	—	—	—
$\angle(C_2C_3C_4)/^\circ$	104.3(2)	104.4(3) ^e	109.7 ^f	104.1	107.9	-	—
$\tau(C_1C_2C_4C_5)/^\circ$	-0.20(54)	-0.73(6) ^e	0.0 ^f	-0.74	-	-	—
$\tau(C_7C_1C_5C_6)/^\circ$	142.0(5)	142.1(8)	-	142.7	—	—	—
$\tau(C_3C_4C_5C_1)/^\circ$	-19.7(11)	-16.6(9)	-	-19.3	-	-	—
$\tau(C_8C_7C_1C_2)/^\circ$	-60.5(6)	-61.4(7)	-	-60.9	—	—	—
$\tau(C_{10}C_4C_3C_2)/^\circ$	-147.5(11)	-148.5(8)	-	-145.3	—	—	—
$\tau(C_4C_5C_6C_1)/^\circ$	-96.4(5)	-95.1(7)	-	-95.3	—	—	—
$\tau(C_5C_4C_3C_2)/^\circ$	-153.48(91)	-153.12(72) ^e	-	-153.13	-	-	—
$\tau(C_1C_2C_4C_3)/^\circ$	153.25(50)	152.39(60) ^e	-	152.39	-	-	—
$\tau(C_2C_1C_5C_6)/^\circ$	-109.40(47)	-110.31(59)	-	-110.32	-	-	—
$\tau(C_4C_5C_1C_6)/^\circ$	109.03(99)	109.13(81) ^e	-	109.13	-	-	—
$\tau(C_1C_6C_7C_8)/^\circ$	-46.6(6)	-45.2(8) ^e	78 ^f	-45.60	—	—	—
$\tau(C_1C_6C_7C_9)/^\circ$	101.9(7)	103.2(9) ^e	-	102.99	—	—	—
$\phi_1^g/^\circ$	26.52(91)	26.88(72) ^e	55	29.33	38.0	22±8	-
$\phi_2^g/^\circ$	26.75(50)	27.61(60) ^e	55	29.33	38.0	22±8	-
$\tau_1^g/^\circ$	70.60(47)	69.69(71) ^e	66.9 ^f	69.29	63.0	66.9 ^f	68.53(4)
$\tau_2^g/^\circ$	70.97(99)	70.97(81) ^e	66.9 ^f	69.29	63.0	66.9 ^f	68.53(4)
$\sigma_{\text{fit}}/ \text{u\AA}^2$	-	0.0091	-	-	-	-	-

^a Ref. 23; ^b Ref. 33; ^c Ref. 34; ^d Non-fitted parameters were fixed to the MP2/6-311++G(d,p) values. ^e parameter not directly fitted, derived from the r_0 Cartesian coordinates. ^f assumed parameters; ^g $\phi_1 = \pi + \tau(C_5C_4C_2C_3)$, $\phi_2 = \pi - \tau(C_1C_2C_4C_3)$, $\tau_1 = \pi + \tau(C_2C_1C_5C_6)$ and $\tau_2 = \pi - \tau(C_4C_5C_1C_6)$.

5. Conclusion

In this work, we have revisited the rotational spectrum of sabinene ($C_{10}H_{16}$) in the 2-20 GHz microwave region, completing the early investigation of Kisiel and Legon.[22] It was analyzed with the help of quantum chemical calculations and using the Kisiel's ($B + C$) sum of constants. Thanks to advances in sensitivity and resolution of Fourier transform microwave spectroscopy coupled to supersonic expansions technique, the spectra of the 10 singly substituted ^{13}C of sabinene were observed in natural abundance. The eleven sets of rotational constants enabled us to calculate a substitution structure and an effective structure limited to the carbon skeleton. The experimental structures as well as the computationally optimized ones are generally in good agreement with each other. The most striking result is the difference in structural parameters between our work and that of Kisiel and Legon. The experimental values of the dihedral angles $\tau \approx 70.9^\circ$ and $\phi \approx 27^\circ$ defining the boat skeleton of the bicyclic structure of sabinene are very far from the early values of $\tau = 66.9^\circ$ (assumed) and ϕ determined to be 55° . The updated structure of sabinene converges towards the structures of compounds based on bicyclo[3.1.0]hexane. It may be useful at the time of analysing vibrational spectra associated with ring-puckering motions.

6. Acknowledgments

The present work was funded by the French ANR Labex CaPPA through the PIA under contract ANR-11-LABX-0005-01, by the Regional Council Hauts de France, by the European Funds for Regional Economic Development (FEDER), and by the French Ministère de l'Enseignement Supérieur et de la Recherche. It is a contribution to the CPER research Project CLIMIBIO.

7. Supplementary Material

Please see the supplementary material for : output of the CORSCL program (scaled constants of the ^{13}C isotopic species, output of the STRFIT program (calculation of the effective structure), the frequencies of the measured lines, structural data of quantum chemical calculations at different levels of the theory.

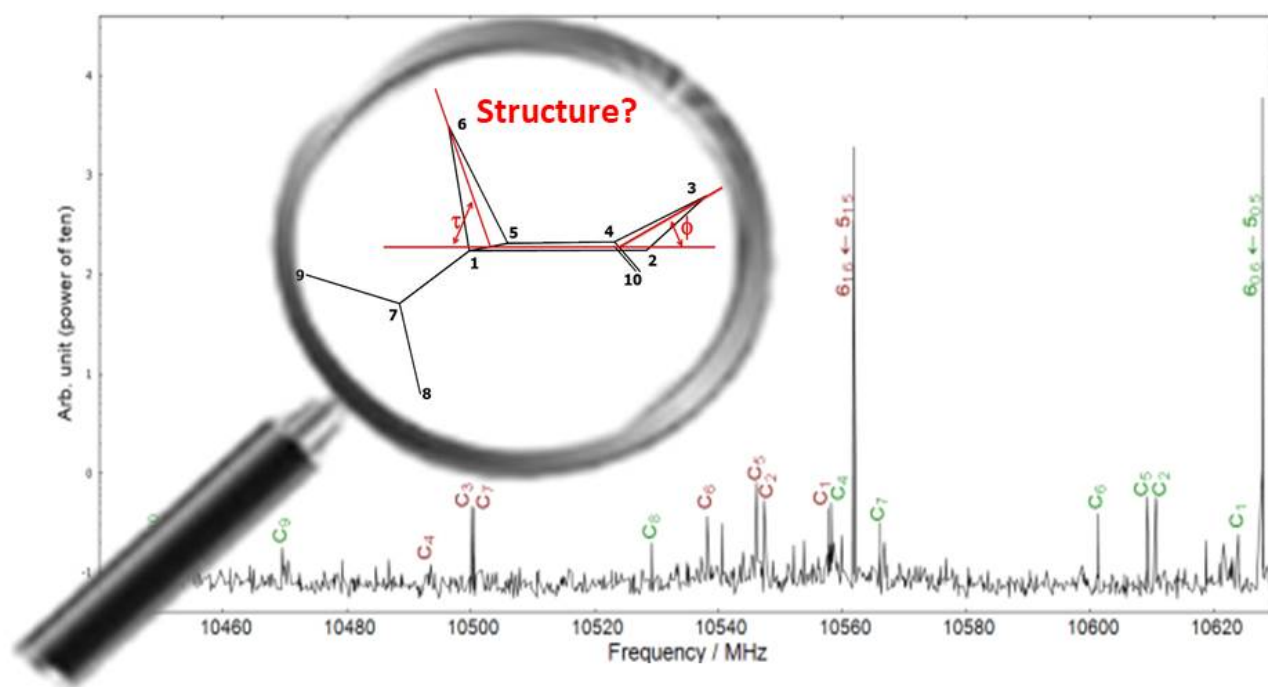


Figure 3: Graphical abstract

References

- [1] E. Breitmaier, Terpenes: Importance, General Structure, and Biosynthesis, John Wiley Sons, Ltd, 2006, Ch. 1, pp. 1–9.
- [2] A. Mutzel, M. Rodigast, Y. Iinuma, O. Böge, H. Herrmann, Monoterpene SOA – contribution of first-generation oxidation products to formation and chemical composition, *Atmos. Environ.* 130 (2016) 136 – 144. doi:10.1016/j.atmosenv.2015.10.080.
- [3] U. Baltensperger, M. Kalberer, J. Dommen, D. Paulsen, M. Alfarra, H. Coe, R. Fisseha, A. Gascho, M. Gysel, S. Nyeki, M. Sax, M. Steinbacher, A. Prevot, S. Sjögren, E. Weingartner, R. Zenobi, Secondary organic aerosols from anthropogenic and biogenic precursors, *Faraday Discuss.* 130 (2005) 265–278. doi:10.1039/b417367h.
- [4] V. Librando, G. Tringali, Atmospheric fate of OH initiated oxidation of terpenes. Reaction mechanism of α -pinene degradation and secondary organic aerosol formation, *J. Environ. Manage.* 75 (2005) 275–282. doi:10.1016/j.jenvman.2005.01.001.
- [5] D. Johnson, G. Marston, The gas-phase ozonolysis of unsaturated volatile organic compounds in the troposphere, *Chem. Soc. Rev.* 37 (2008) 699–716. doi:10.1039/b704260b.
- [6] D. Aljawhary, R. Zhao, A. Lee, C. Wang, J. Abbatt, Kinetics, mechanism, and secondary organic aerosol yield of aqueous phase photo-oxidation of α -pinene oxidation products, *J. Phys. Chem. A* 120 (2016) 1395–1407. doi:10.1021/acs.jpca.5b06237.
- [7] L. Vereecken, J. Peeters, A theoretical study of the OH-initiated gas-phase oxidation mechanism of β -pinene ($C_{10}H_{16}$): first generation products, *Phys. Chem. Chem. Phys.* 14 (2012) 3802–3815. doi:10.1039/c2cp23711c.

- [8] W. Miekisch, J. K. Schubert, G. F. Noeldge-Schomburg, Diagnostic potential of breath analysis—focus on volatile organic compounds, *Clin. Chim. Acta* 347 (2004) 25–39. doi:10.1016/j.cccn.2004.04.023.
- [9] L. Tollsten, P. M. Müller, Volatile organic compounds emitted from beech leaves, *Phytochemistry* 43 (1996) 759–762. doi:10.1016/0031-9422(96)00272-5.
- [10] S. Owen, C. Boissard, R. Street, S. Duckham, O. Csiky, C. Hewitt, Screening of 18 mediterranean plant species for volatile organic compound emissions, *Atmos. Environ.* 31 (1997) 101–117. doi:10.1016/S1352-2310(97)00078-2.
- [11] R. A. Street, S. Owen, S. C. Duckham, C. Boissard, C. N. Hewitt, Effect of habitat and age on variations in volatile organic compound (VOC) emissions from *Quercus ilex* and *Pinus pinea*, *Atmos. Environ.* 31 (1997) 89–100. doi:10.1016/S1352-2310(97)00077-0.
- [12] J. H. Seinfeld, J. F. Pankow, Organic atmospheric particulate material, *Annu. Rev. Phys. Chem.* 54 (2003) 121–140. doi:10.1146/annurev.physchem.54.011002.103756.
- [13] M. Almatarneh, I. Elayan, M. Altarawneh, J. Hollett, A computational study of the ozonolysis of sabinene, *Theor. Chem. Acc.* 138 (2019) 1–14. doi:10.1007/s00214-019-2420-7.
- [14] N. Carrasco, M. T. Rayez, J. C. Rayez, J. F. Doussin, Experimental and theoretical study of the reaction of OH radical with sabinene, *Phys. Chem. Chem. Phys.* 8 (2006) 3211–3217. doi:10.1039/B604489A.
- [15] Y. Zhao, R. Zhang, H. Wang, M. He, X. Sun, Q. Zhang, W. Wang, M. Ru, Mechanism of atmospheric ozonolysis of sabinene: a DFT study, *Comput. Theor. Chem.* 942 (2010) 32–37. doi:10.1016/j.theochem.2009.11.029.
- [16] R. J. Griffin, D. R. Cocker III, R. C. Flagan, J. H. Seinfeld, Organic aerosol formation from the oxidation of biogenic hydrocarbons, *J. Geophys. Res.* 104 (1999) 3555–3567. doi:10.1029/1998JD100049.
- [17] J. F. Pankow, J. H. Seinfeld, W. E. Asher, G. B. Erdakos, Modeling the formation of secondary organic aerosol. 1. Application of theoretical principles to measurements obtained in the α -pinene/, β -pinene/, sabinene/, Δ^3 -carene/, and cyclohexene/ozone systems, *Environ. Sci. Technol.* 35 (2001) 1164–1172. doi:10.1021/es001321d.
- [18] F. Bernard, I. Fedioun, F. Peyroux, A. Quilgars, V. Daële, A. Mellouki, Thresholds of secondary organic aerosol formation by ozonolysis of monoterpenes measured in a laminar flow aerosol reactor, *J. Aerosol Sci.* 43 (2012) 14–30. doi:10.1016/j.jaerosci.2011.08.005.
- [19] J. Valente, M. Zuzarte, M. Gonçalves, M. Lopes, C. Cavaleiro, L. Salgueiro, M. Cruz, Antifungal, antioxidant and anti-inflammatory activities of *Oenanthe crocata* L. essential oil, *Food Chem. Toxicol.* 62 (2013) 349–354. doi:10.1016/j.fct.2013.08.083.
- [20] Y. Cao, H. Zhang, H. Liu, W. Liu, R. Zhang, M. Xian, H. Liu, Biosynthesis and production of sabinene: current state and perspectives, *Appl. Microbiol. Biotechnol.* 102 (2018) 1535–1544. doi:10.1007/s00253-017-8695-5.
- [21] A. N. Menon, K. P. Padmakumari, Studies on essential oil composition of cultivars of black pepper (*Piper nigrum* L.)-V, *J. Essent. Oil Res.* 17 (2005) 153–155. doi:10.1080/10412905.2005.9698862.
- [22] Z. Kisiel, A. C. Legon, Conformations of some bicyclic monoterpenes based on bicyclo [3.1.0] hexane from their low-resolution microwave spectra, *J. Am. Chem. Soc.* 100 (1978) 8166–8169. doi:10.1021/ja00494a024.
- [23] R. L. Cook, T. Malloy, Microwave spectrum, dipole moment, and conformation of bicyclo [3.1.0] hexane, *J. Am. Chem. Soc.* 96 (1974) 1703–1707. doi:10.1021/ja00813a010.

- [24] J. W. Bevan, A. C. Legon, S. O. Ljunggren, P. J. Mjoberg, Microwave spectrum, molecular geometry, ring bending potential function, and electric dipole moment of bicyclo [3.1.0] hexan-3-one, *J. Am. Chem. Soc.* 100 (1978) 8161–8165. doi:10.1021/ja00494a023.
- [25] E. J. Ocola, L. A. Wieding, S. Adams, J. Laane, Theoretical study of structures and ring-puckering potential energy functions of bicyclo [3.1.0] hexane and related molecules, *J. Phys. Chem. A* 122 (2018) 5970–5977. doi:10.1021/acs.jpca.8b04930.
- [26] D. Loru, M. A. Bermúdez, M. E. Sanz, Structure of fenchone by broadband rotational spectroscopy, *J. Chem. Phys.* 145 (2016) 1627–1638. doi:10.1063/1.4961018.
- [27] Z. Kisiel, O. Desyatnyk, E. Białkowska-Jaworska, L. Pszczołkowski, The structure and electric dipole moment of camphor determined by rotational spectroscopy, *Phys. Chem. Chem. Phys.* 5 (2003) 820–826. doi:10.1039/b212029a.
- [28] E. Neeman, P. Dréan, T. Huet, The structure and molecular parameters of camphene determined by Fourier transform microwave spectroscopy and quantum chemical calculations, *J. Mol. Spectrosc.* 322 (2016) 50–54. doi:10.1016/j.jms.2016.03.012.
- [29] E. M. Neeman, J. R. Avilés Moreno, T. R. Huet, The gas phase structure of α -pinene, a main biogenic volatile organic compound, *J. Chem. Phys.* 147 (2017) 214305. doi:10.1063/1.5003726.
- [30] E. M. Neeman, J. R. Avilés-Moreno, T. R. Huet, The quasi-unchanged gas-phase molecular structures of the atmospheric aerosol precursor β -pinene and its oxidation product nopinone, *Phys. Chem. Chem. Phys.* 19 (2017) 13819–13827. doi:10.1039/c7cp01298e.
- [31] M. Chrayteh, P. Dréan, T. Huet, Structure determination of myrtenal by microwave spectroscopy and quantum chemical calculations, *J. Mol. Spectrosc.* 336 (2017) 22–28. doi:10.1016/j.jms.2017.04.005.
- [32] F. E. Marshall, G. Sedo, C. West, B. H. Pate, S. M. Allpress, C. J. Evans, P. D. Godfrey, D. McNaughton, G. S. Grubbs II, The rotational spectrum and complete heavy atom structure of the chiral molecule verbenone, *J. Mol. Spectrosc.* 342 (2017) 109–115. doi:10.1016/j.jms.2017.09.003.
- [33] A. Davies, A. Legon, D. Millen, A. Roberts, Microwave rotational spectrum, electric dipole moment and geometry of 2-bicyclo[3.1.0] hexanone, *J. Mol. Struct.* 112 (1984) 9–18. doi:10.1016/0022-2860(84)80238-0.
- [34] S. Bomar, E. Bay, H.-G. Kraft, J. W. Bevan, The microwave spectrum of 2,4-dioxabicyclo [3.1.0] hexan-3-one, *J. Mol. Spectrosc.* 87 (1981) 482–489. doi:10.1016/0022-2852(81)90419-7.
- [35] M. J. Frisch, G. W. Trucks, H. B. Schlegel, G. E. Scuseria, M. A. Robb, J. R. Cheeseman, G. Scalmani, V. Barone, G. A. Petersson, H. Nakatsuji, X. Li, M. Caricato, A. V. Marenich, J. Bloino, B. G. Janesko, R. Gomperts, B. Mennucci, H. P. Hratchian, J. V. Ortiz, A. F. Izmaylov, J. L. Sonnenberg, D. Williams-Young, F. Ding, F. Lipparini, F. Egidi, J. Goings, B. Peng, A. Petrone, T. Henderson, D. Ranasinghe, V. G. Zakrzewski, J. Gao, N. Rega, G. Zheng, W. Liang, M. Hada, M. Ehara, K. Toyota, R. Fukuda, J. Hasegawa, M. Ishida, T. Nakajima, Y. Honda, O. Kitao, H. Nakai, T. Vreven, K. Throssell, J. A. Montgomery, Jr., J. E. Peralta, F. Ogliaro, M. J. Bearpark, J. J. Heyd, E. N. Brothers, K. N. Kudin, V. N. Staroverov, T. A. Keith, R. Kobayashi, J. Normand, K. Raghavachari, A. P. Rendell, J. C. Burant, S. S. Iyengar, J. Tomasi, M. Cossi, J. M. Millam, M. Klene, C. Adamo, R. Cammi, J. W. Ochterski, R. L. Martin, K. Morokuma, O. Farkas, J. B. Foresman, D. J. Fox, Gaussian 16 Revision B.01, gaussian Inc. Wallingford CT (2016).
- [36] C. Lee, W. Yang, R. G. Parr, Development of the Colle-Salvetti correlation-energy formula into a functional of the electron density, *Phys. Rev. B* 37 (1988) 785–789. doi:10.1103/PhysRevB.37.785.

- [37] Y. Zhao, D. G. Truhlar, The M06 suite of density functionals for main group thermochemistry, thermochemical kinetics, noncovalent interactions, excited states, and transition elements: two new functionals and systematic testing of four M06-class functionals and 12 other functionals, *Theor. Chem. Acc.* 120 (2008) 215–241. doi:10.1007/s00214-007-0310-x.
- [38] C. Møller, M. S. Plesset, Note on an approximation treatment for many-electron systems, *Phys. Rev.* 46 (1934) 618–622. doi:10.1103/PhysRev.46.618.
- [39] S. Kassi, D. Petitprez, G. Wlodarczak, Microwave Fourier transform spectroscopy of t-butylchloride and t-butylbromide isotopic species, *J. Mol. Struct.* 517-518 (2000) 375 – 386. doi:10.1016/S0022-2860(99)00296-3.
- [40] M. Tudorie, L. H. Coudert, T. R. Huet, D. Jegouso, G. Sedes, Magnetic hyperfine coupling of a methyl group undergoing internal rotation: a case study of methyl formate, *J. Chem. Phys.* 134 (2011) 074314. doi:10.1063/1.3554419.
- [41] S. Kassi, D. Petitprez, G. Wlodarczak, Microwave spectrum of isotopic species of urea (NH₂)₂CO, *J. Mol. Spectrosc.* 228 (2004) 293–297. doi:10.1016/j.jms.2004.05.002.
- [42] H. Pickett, The fitting and prediction of vibration-rotation spectra with spin interactions, *J. Mol. Spectrosc.* 148 (1991) 371–377. doi:10.1016/0022-2852(91)90393-0.
- [43] Z. Kisiel, *Spectroscopy from Space*, Kluwer Academic Publishers, Dordrecht, 2001, pp. 91–106.
- [44] J. Kraitchman, Determination of molecular structure from microwave spectroscopic data, *Am. J. Phys.* 21 (1953) 17–24. doi:10.1119/1.1933338.
- [45] Z. Kisiel, Prospe - programs for ROtational SPEctroscopy, <http://www.ifpan.edu.pl/~kisiel/prospe.htm>, accessed: 2021-02-10.
- [46] C. C. Costain, Further comments on the accuracy of r_s substitution structures, *Trans. Am. Crystallogr. Assoc.* 2 (1966) 157–164.
- [47] A. J. Minei, S. A. Cooke, Evaluation of the substitution structures of two partially fluorinated cyclopentanes C₅H₃F₇ and C₅H₂F₈, *J. Mol. Struct.* 1207 (2020) 127778. doi:10.1016/j.molstruc.2020.127778.
- [48] J. Demaison, H. Rudolph, When is the substitution structure not reliable?, *J. Mol. Spectrosc.* 215 (2002) 78–84. doi:10.1006/jmsp.2002.8610.
- [49] Z. Kisiel, Least-squares mass-dependence molecular structures for selected weakly bound intermolecular clusters, *J. Mol. Spectrosc.* 218 (2003) 58–67. doi:10.1016/S0022-2852(02)00036-X.